Journal of Applied Mechanics and Technical Physics, Vol. 37, No. 6, 1996

EXPERIMENTS WITH SHALLOW-WATER WAVES GENERATED BY THE MOTION OF THE SIDE WALL OF A CHANNEL

V. I. Bukreev and N. P. Turanov

UDC 532.59

A prismatic channel with a rectangular cross section and a horizontal bottom of length L and width B is filled with water at rest to depth h. At moment $t = 0$, one of the side walls begins to be displaced by a specified law. The forces acting on the wall and the wave motion in the channel are the subject of interest. This paper presents the results of experimental study of waves, focusing exclusively on gravity waves.

If we confine ourselves to consideration of plane waves and the time interval before the arrival of reflected waves at a given point in space and ignore the effect of air, surface tension, viscosity, and compressibility of water, the undisturbed state of a dynamic system can be characterized by three parameters: depth h, acceleration of gravity g, and water density ρ. The kinematic properties of the waves depend on h and g, while ρ plays a significant part only in analysis of forces. Without additional information on the perturbation introduced into the system, none of the dimensionless complexes of these quantities can be constructed.

There are, however, at least two critical velocities [1], $c_* = \sqrt{gh}$ and $c_{**} = \sqrt{2gh}$, in the vicinity of which one should expect qualitative changes in the gravity-wave pattern, whatever the method of their generation. In particular, c_* limits the region of existence of stationary harmonic waves, and c_{**} limits the region of existence of cnoidal waves (including solitary ones) [1]. The motion of a side wall is an attractive method of wave generation due to the possibility of introducing perturbations, whose velocities are far higher than the critical ones. It should also be noted that the problem of shallow-water gravity waves is, in a sense, similar to the fundamental problem of gas dynamics on the motion of a piston in a tube [2].

The previous experiments dealt mainly with two applied problems. One problem concerns the action force of a liquid on a wall [3]. The second one is mainly the problem of a wavemaker, and it can be thought to be inverse to the problem with which we deal here — to find such a law of the motion of a wall which ensures the formation of waves of a specified form. One of the major achievements in this line of research is practical realization of the process of wave breaking in a given section of the channel [4].

Studies of the theoretical and computational character are based on the potential fluid motion model, while in analytical studies the method of small-parameter expansion is used. A small parameter is usually either the ratio of water depth to wave length (the shallow water theory) [2], or dimensionless time [5], or the ratio between the wave amplitude and length [6]. In recent years, many numerical experiments based on the model of potential motion have been performed (see, for example, [7, 8]). It is worth noting the so-called discrete incompressible-fluid model [9], which is well adapted to numerical experiments. Valuable information on the problems considered below is given in [10].

On the whole, modern mathematical models adequately describe physical processes only in a limited range of parameters. Their application becomes particularly difficult in the case of wave breaking at supercritical velocities when the energy strongly dissipates, and the fluid becomes two-phase. One has managed to reproduce only the initial stage of the process of wave breaking in numerical experiments.

In the present work, several dozen partial solutions of the problem considered are obtained for combinations of the parameters that make it possible to describe well the wave motions by modern analytical

Lavrent'ev Institute of Hydrodynamics, Siberian Division, Russian Academy of Sciences, Novosibirsk 630090. Translated from Prikladnaya Mekhanika i Tekhnicheskaya Fizika, Vol. 37, No. 6, pp. 44–50, November–December, 1996. Original article submitted September 13, 1995.

 0021-8944/96/3706-0810 $15.00

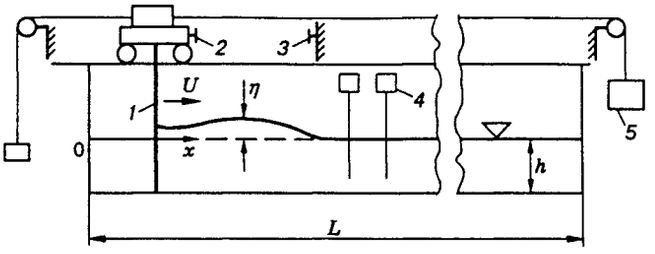

Fig. 1

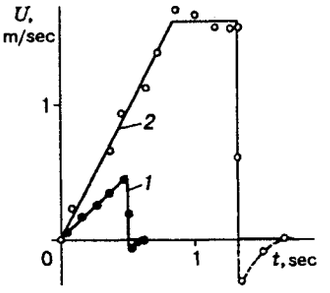

Fig. 2

and numerical methods and also at supercritical perturbation velocities. The length of the channel in the experiments is limited, and when the time t is large, the parameter L plays a significant part. In the case of wave breaking, the effect of the viscosity and compressibility of air and water, surface tension, and the difference in water and air densities is of great importance.

The experimental setup is schematically shown in Fig. 1. A plane vertical plate 1 totally blocking the channel cross section was set in motion by a carriage 2 driven concurrently by an electric motor and by a falling weight 5. Having passed a specified path S, the carriage was stopped abruptly by a grip 3. This made it possible to realize with acceptable accuracy one of the simplest, in number of parameters, laws of motion: constant acceleration within the time interval $(0, T_1]$, uniform motion with velocity U_0 in the interval $(T_1, T_2]$, and an abrupt stop at $t = T_2$.

Figure 2 shows two examples of the law of motion of a wall. The time t is plotted along the abscissa from the moment of start, and the carriage velocity U is plotted along the ordinate. The experimental points are obtained by numerical differentiation of the signal from a rheochord transducer, which registered the motion of the carriage $s(t)$. The curves correspond to the following approximation:

$$U = \begin{cases} at & \text{for} \quad 0 \leqslant t < T_1, \\ U_0 & \text{for} \quad T_1 \leqslant t < T_2, \\ 0 & \text{for} \quad t \geqslant T_2, \end{cases} \tag{1}$$

where a, T_1, $U_0 = aT_1$, and T_2 are the parameters. For curve 1, $T_2 = T_1$, and the law of motion is characterized only by two parameters: a and T_1 (or U_0) [$a = 96$ cm/sec^2 and $T_1 = 0.5$ sec ($U_0 = 48$ cm/sec)]. Curve 2 is described by three parameters: $a = 196$ cm/sec^2, $T_1 = 0.82$ sec, and $T_2 = 1.32$ sec ($U_0 = 161$ cm/sec).

Because of the elasticity of mechanical systems, it is impossible in the experiment to stop the wall instantaneously. Moreover, this is undesirable when gravity waves are studied. Due to the elasticity of the grip and other parts, after the stoppage the carriage moved back a little with a velocity that is significantly less than U_0. This is indicated in Fig. 2 by the fact that the velocity U assumes negative values for $t > T_2$. The length of a path that is covered by the wall in backward motion did not exceed 1% of S. It is assumed that such a deviation from approximation (1) exerted no significant effect on the inertial gravity waves.

The parameter B was equal to 20 cm, and the parameters h, a, T_1, T_2, and L were varied. Deviations of the free surface from equilibrium η were measured by wavemeters 4 (see Fig. 1). Below, we give the results of measurements with fixed wavemeters which registered $\eta(t)$ at given values of the longitudinal coordinate x (the fixed x axis is shown in Fig. 1). Additional information was obtained by means of wavemeters fastened to the carriage along with photographic recording. The perturbation velocity c was estimated by signals from two wavemeters spaced $\Delta x \leqslant 30h$ apart.

In the experiments, attention was focused on two fundamental questions. Can the perturbation propagate with a supercritical velocity? If yes, does it remain stable in such a propagation? The instability of gravity waves manifests itself as wave breaking.

In the hydrodynamic problem under consideration, a positive answer to the first question follows from the law of conservation of mass and, hence, the perturbation can be realized for practically unlimited values

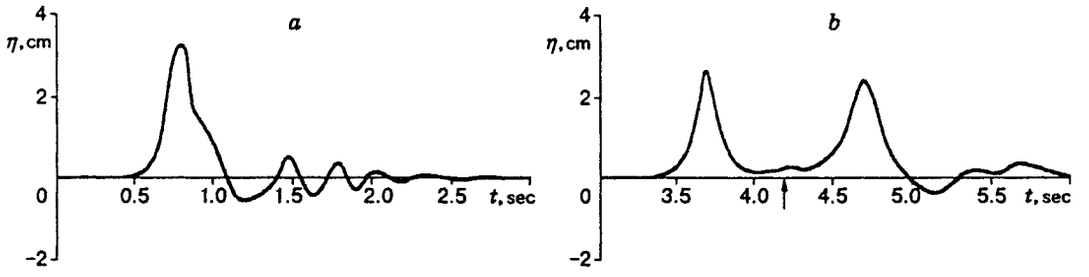

Fig. 3

of c. The gravity field hinders the vertical rise of the fluid displaced by the wall, whereas there is no such limitation along the x axis, provided that $L \to \infty$. In all the experiments, the perturbation's leading edge overtook the moving wall, irrespective of whether the latter moved with a subcritical or supercritical velocity. For a sufficiently large U_0, the propagation velocity c was significantly larger than c_{**}.

Perturbation stability is a more complicated problem. It was studied well enough for $c < c_{**}$. In particular, there are smooth stable singular waves in the range $c_* < c < c_{**}$. Let us present another example of a smooth stable wave for which c is larger than c_* but smaller than c_{**}. In this example, the wave differs from a solitary wave — it is nonsteady. In this wave, the effect of dispersion prevails over that of nonlinearity, and this determines the wave stability. Another stabilizing factor is water viscosity.

The wave just described was obtained at $h = 4.9$ cm and for values of a, T_1, and T_2 corresponding to curve 1 in Fig. 2. Figure 3 shows the wave as a function of t for $x_1 = 42$ cm (a) and $x_2 = 297$ cm (b). The arrow shows the moment of arrival of the wave reflected from the fixed side wall for which $x_3 = L = 336$ cm.

The perturbation in question is unsteady. For this perturbation, the quantity c is defined as the velocity of a point of the wave-front slope that departed upward from the equilibrium point by the magnitude $\eta_{0.5} = \eta_m/2$ (η_m is the height of the first crest). It should be noted that all the other points of the front slope in this example moved with a velocity which differed from c by not more than 5%. However, for stability, it is important to know exactly which points move faster — those at the top or those at the foot of the crest. For the perturbation in Fig. 3, the points at the foot moved faster and the wave was stable.

In Fig. 3a, the wave is strongly nonsymmetric, and $c = 83.3$ cm/sec $= 1.202c_* = 0.850c_{**}$. The high front crest is followed by a train of almost periodically decreasing (in amplitude) waves. The level of the back slope of the first crest decreases nonmonotonically. With an increase in x, the perturbation tends to take the shape of a solitary wave, but in the case considered it fails. This is due, to a considerable extent, to the water viscosity which violates the balance between the nonlinearity and dispersion effects. As a result, the wave remains unsteady up to complete degeneration.

For $x_2 = 60.6h$ (Fig. 3b), the fixed wavemeter registers a pair of high crests. The first is a leading wave which propagates in the fluid at rest, and the second is a reflected wave which propagates in a slightly perturbed fluid. The properties of the leading wave are close to those of the solitary wave. For the direct wave, $c = 88.2$ cm/sec $= 1.272c_* = 0.900c_{**}$, i.e., slightly larger than in the case of Fig. 3a. This means that after the wall had stopped, the wave continued to gain speed and then began to decelerate because of dispersion and viscosity. Subsequently, i.e., after the moments indicated in Fig. 3b, the value of c slowly decreased. The value of $c = c_*$ was reached when the path was approximately equal to $500h$, the wave having reflected 6 times from the fixed vertical walls. Reflections did not affect the stability, and the wave height and propagation velocity changed insignificantly.

There is no arguing that mathematical models based on the Navier–Stokes equations can describe this example with better accuracy and in more detail than can be done in experiments. To test simpler mathematical models and numerical methods, we give in Tables 1 and 2 the experimental values of η (Table 1 corresponds to Fig. 3a, and Table 2 to Fig. 3b).

For $c > c_{**}$, the perturbations were unstable, and their front slope broke. If c was not much larger than c_{**}, breaking did not occur immediately. We had an example in which the unsteady wave remained smooth up

TABLE 1

t, sec	η, cm	t, sec	η, cm	t, sec	η, cm	t, sec	η, cm
0.40	0	1.30	−0.40	7.50	0.06	8.93	−0.25
0.42	0	1.40	0.02	7.60	0.40	9.00	−0.15
0.50	0.05	1.46	0.47	7.71	1.85	9.10	0.15
0.60	0.30	1.50	0.32	7.77	2.27	9.20	0.37
0.65	0.77	1.60	−0.38	7.81	1.86	9.30	0.43
0.72	2.17	1.65	−0.38	7.90	0.58	9.40	0.35
0.76	3.12	1.70	−0.12	8.00	0.14	9.50	0.16
0.77	3.22	1.77	0.31	8.10	0.10	9.60	0.04
0.78	3.24	1.80	0.26	8.20	0.11	9.70	−0.04
0.79	3.17	1.85	−0.07	8.30	0.27	9.80	−0.01
0.83	2.98	1.90	−0.29	8.40	0.72	9.90	0.05
0.86	1.76	1.95	−0.12	8.51	1.76	10.00	0.20
0.91	1.45	2.00	0.09	8.55	1.90	10.10	0.17
0.95	1.17	2.50	0.09	8.61	1.64	10.20	0.10
1.00	0.81	3.00	−0.12	8.70	0.64	10.30	0
1.10	−0.21	7.40	0	8.80	0.02	10.40	−0.02
1.20	−0.62	7.43	0	8.90	−0.24	10.50	−0.11

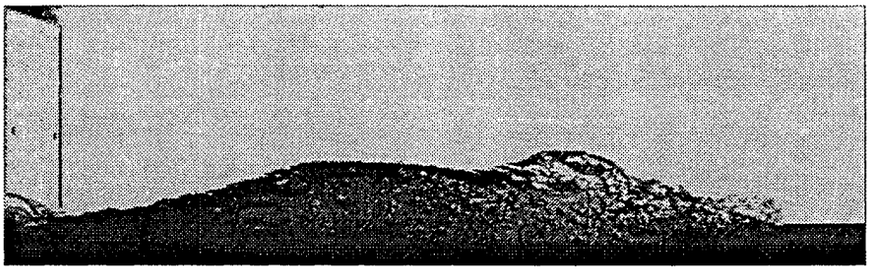

Fig. 4

to a distance of as much as $50h$ from the moving wall. Upon intense perturbation, breaking occurred directly near the moving wall. There were cases where breaking occurred not only at the front slope of the wave but also at the back one.

Figure 4 shows a photograph of the perturbation for $h = 1$ cm and $L = 392$ cm, with the values of a, T_1, and T_2 corresponding to curve 2 in Fig. 2. The exposure time ranged from 1/500 sec to approximately 0.1 sec after the wall had stopped. The wave propagated from left to right. It is noteworthy that there is a breaker and a pit on the wave crest, while the back slope of the wave is unstable.

Further evolution of this perturbation is illustrated by Fig. 5, which shows the function $\eta(t)$ for a fixed difference $x - S = 75$ cm ($S = 146.5$ cm) and where 1 is the leading wave propagating in the fluid at rest for $c_1 = 161.3$ cm/sec $= 5.15c_* = 3.63c_{**}$ and 2–5 are reflected waves (the odd numbers designate the waves moving in the positive direction x and the even numbers refer to the waves moving in the negative direction). For wave 2, $c_2 = 62.5$ cm/sec and the water depth ahead of its front is almost zero. In this case, the concepts of c_* and c_{**} lose their significance, and the typical velocity can be determined as $c_{***} = \sqrt{2gH}$ (H is the water depth behind the wave). It turned out that $c_2 \cong c_{***}$. Waves 3–5 propagated with almost equal velocities ($c_3 = 34.1$, $c_4 = 36.6$, and $c_5 = 32.6$ cm/sec). The water depth before their fronts was not constant, and their critical velocities are indeterminate.

Figure 5b–d shows waves 1, 2, and 5 on a larger scale. Waves 1–3 were unstable and broke. Wave 4 and all subsequent waves were stable and smooth. Wave 5 is similar in shape to the so-called undular wave.

TABLE 2

t, sec	η, cm	t, sec	η, cm	t, sec	η, cm	t, sec	η, cm
3.22	0	4.23	0.23	5.20	−0.31	6.75	0.06
3.32	0.01	4.30	0.20	5.30	0.02	6.86	0.23
3.42	0.08	4.35	0.22	5.40	0.15	6.95	0.12
3.50	0.23	4.40	0.33	5.50	0.10	7.05	−0.05
3.55	0.55	4.50	0.64	5.53	0.10	7.13	−0.10
3.61	1.26	4.56	1.00	5.60	0.26	7.20	−0.06
3.64	2.00	4.61	1.66	5.70	0.48	7.30	0.01
3.67	2.54	4.65	2.12	5.80	0.29	7.40	0
3.72	2.00	4.69	2.32	5.90	0.14	7.50	0
3.76	1.30	4.74	2.00	6.00	0	7.60	0.09
3.80	0.74	4.81	1.12	6.08	−0.10	7.72	0.19
3.85	0.37	4.85	0.62	6.17	0	7.80	0.06
3.90	0.19	4.90	0.30	6.26	0.05	7.93	−0.20
3.95	0.14	4.95	0.07	6.36	0	8.00	−0.12
4.00	0.12	5.00	−0.11	6.44	−0.11	8.10	0.20
4.10	0.12	5.10	−0.37	6.55	−0.30	8.15	0.28
4.20	0.22	5.15	−0.41	6.65	−0.20	8.27	0

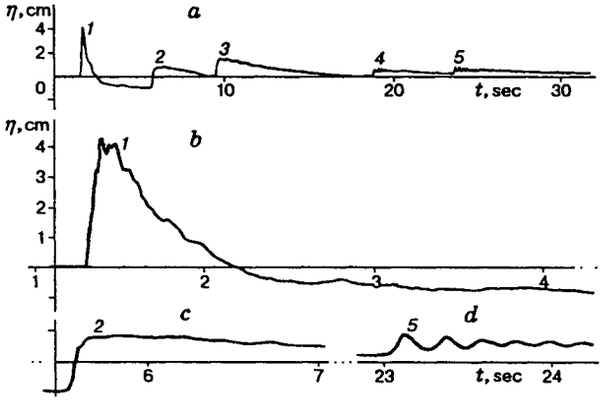

Fig. 5

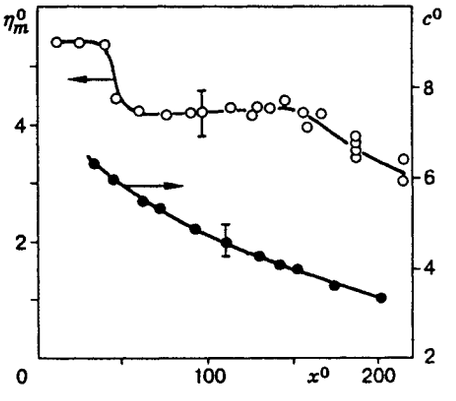

Fig. 6

Owing to intense energy dissipation, the height and propagation velocity of unstable waves decrease with time much faster than those of stable waves. Figure 6 shows the curves of the dimensionless height $\eta_m^0 = \eta_m/h$ and dimensionless velocity $c^0 = c_1/\sqrt{gh}$ of wave 1 versus $x^0 = (x - S)/h$. The velocity c^0 decreases monotonically. The height η_m^0 diminishes abruptly in the vicinity of $x^0 = 42$, remains practically constant up to $x^0 \cong 140$, and only then decreases monotonically. A reference to Fig. 4 will help us to explain such behavior of the wave. In the vicinity of $x^0 = 42$, the breaker at the crest disappears, while for $x^0 < 140$, a wave that decreases the level reaches a wave that increases the level, and the water depth between the two remains unchanged.

On the whole, the experiments have shown that with the above law of motion of the wall, the perturbations introduced by the wall are unstable if $c > c_{**}$. For such perturbations, the stability can be preserved only in a limited time interval due to the nonsteadiness. To realize long-living stable perturbations with $c > c_{**}$, if such exist at all, one needs to employ a different method of introducing perturbations.

An analysis [2] of the problem of dam breaking within the framework of a first approximation of the shallow-water theory yielded a smooth solution for the wave over a dry bottom with the leading-edge

propagation velocity equal to $2\sqrt{gH}$. In the above experiments, wave 2 in Fig. 5 propagated over a dry bottom with the smaller velocity $\sqrt{2gH}$ and was unstable.

We express our gratitude to N. I. Makarenko for useful discussions of the work. In particular, he noted that the numerical results based on the exact model of the potential fluid motion yield for the second critical velocity the value $1.29\sqrt{gh}$, which is somewhat smaller than the value $\sqrt{2gh}$ obtained in a second approximation of the shallow water theory. He also noted that for the unsteady wave in Fig. 3, $c \cong 1.04\sqrt{g(h+\eta_m/2)}$. This value differs little from the local perturbation velocity and agrees with the known solution of the gas-dynamic problem on the accelerated motion of a piston.

This work was supported by the Russian Foundation for Fundamental Research (Grant 95-01-01164a).

REFERENCES

1. L. V. Ovsyannikov, N. I. Makarenko, V. I. Nalimov, et al., *Nonlinear Problems of the Theory of Surface and Internal Waves* [in Russian], Nauka, Novosibirsk (1985).
2. J. J. Stoker, *Water Waves. Mathematical Theory and Applications*, Interscience Publishers, New York (1957).
3. E. S. Chan and W. K. Melville, "Deep-water plunging wave pressure on a vertical plane wall," *Proc. R. Soc. London*, **A417**, No. 1852, 95–131 (1988).
4. D. G. Dommermuth, D. K. P. Yue, E. S. Chan, and W. K. Melville, "Deep-water plunging breakers: a comparison between potential theory and experiments," *J. Fluid Mech.*, **189**, 423–442 (1988).
5. A. T. Chwang, "Nonlinear hydrodynamic pressure on an accelerating plate," *Phys. Fluids*, **26**, No. 2, 383–387 (1983).
6. S. W. Joo, W. W. Schultz, and A. F. Messiter, "An analysis of the initial value wavemaker problem," *J. Fluid. Mech.*, **214**, 161–183 (1990).
7. W. W. Schultz, S. E. Ramberg, and O. M. Griffin, "Steep and breaking deep-water waves," in: Proc. of 16th Symp. Naval Hydrodynamics, Berkeley (1986).
8. M. Miyata, C. Matusukawa, and H. Kajitani, "Shallow water flow with separation and breaking wave," *J. Soc. Naval Architects Jpn.*, **158** (1985).
9. A. M. Frank, "Discrete nonlinear-dispersion shallow-water model," *Prikl. Mekh. Tekh. Fiz.*, **35**, No. 1, 34–42 (1994).
10. M. S. Longuett-Higgins, "Breaking waves in deep or shallow water," in: Proc. of 10th Symp. on Naval Hydrodynamics, Cambridge (1974), pp. 597–605.